A PRELIMINARY DAMAGE TOLERANCE METHODOLOGY FOR COMPOSITE STRUCTURES

D. J. Wilkins
General Dynamics
Fort Worth, Texas

PREVIEW

The work described in this presentation was supported by the F-16 Airplane System Program Office, Aeronautical Systems Division, United States Air Force, as part of the F-16 Production Fleet Management Program. As indicated in Figure 1, the presentation will briefly explore General Dynamics' certification experience for the primary, safety-of-flight composite structure applications on the F-16, will describe the rationale for the selection of delamination as the major issue for damage tolerance, and will outline the modeling approach selected. The development of the necessary coupon-level data base will be referred to and briefly summarized. The major emphasis will be the description of a full-scale test where delamination growth was obtained with which to demonstrate the validity of the selected approach. A summary will be used to review the generic features of the methodology.

- CERTIFICATION EXPERIENCE
- DELAMINATION RATIONALE
- MODELING APPROACH
- DATA BASE DEVELOPMENT
- FULL-SCALE VERIFICATION
- SUMMARY

Figure 1

DEFINE THE WORDS

The Air Force, in MIL-STD-1530A, Airplane Structural Integrity Program, sets forth specific definitions of the words "durability" and "damage tolerance." For the purpose of this presentation, the definitions are given in Figure 2.

DURABILITY	THE ABILITY OF THE AIRFRAME TO RESIST CRACKING, CORROSION, THERMAL DEGRADATION, DELAMINATION, WEAR, AND THE EFFECTS OF FOREIGN OBJECT DAMAGE FOR A SPECIFIED PERIOD OF TIME
DAMAGE TOLERANCE	THE ABILITY OF THE AIRFRAME TO RESIST FAILURE DUE TO THE PRESENCE OF FLAWS, CRACKS, OR OTHER DAMAGE FOR A SPECIFIED PERIOD OF TIME

Figure 2

CERTIFY COMPOSITES BY TEST

In contrast to the combined analysis/test procedures used to certify metallic parts on the F-16, the composite primary structure parts had to be certified completely by test (Figure 3). Full-scale room temperature, dry static and fatigue tests of the vertical tail and the horizontal tail were supplemented with beam tests representing critical load paths. Beams were tested statically at environmental conditions ranging from cold, dry to hot, wet. Coupled load/environment fatigue tests were also performed. All of these tests were necessarily defined only in terms of the contractually specified "design usage."

For reference, the vertical tail employs thick graphite-epoxy skins bolted to aluminum spars and ribs, and the horizontal tail uses graphite-epoxy skins bonded to full-depth aluminum honeycomb core and bolted to a titanium hub/spar substructure.

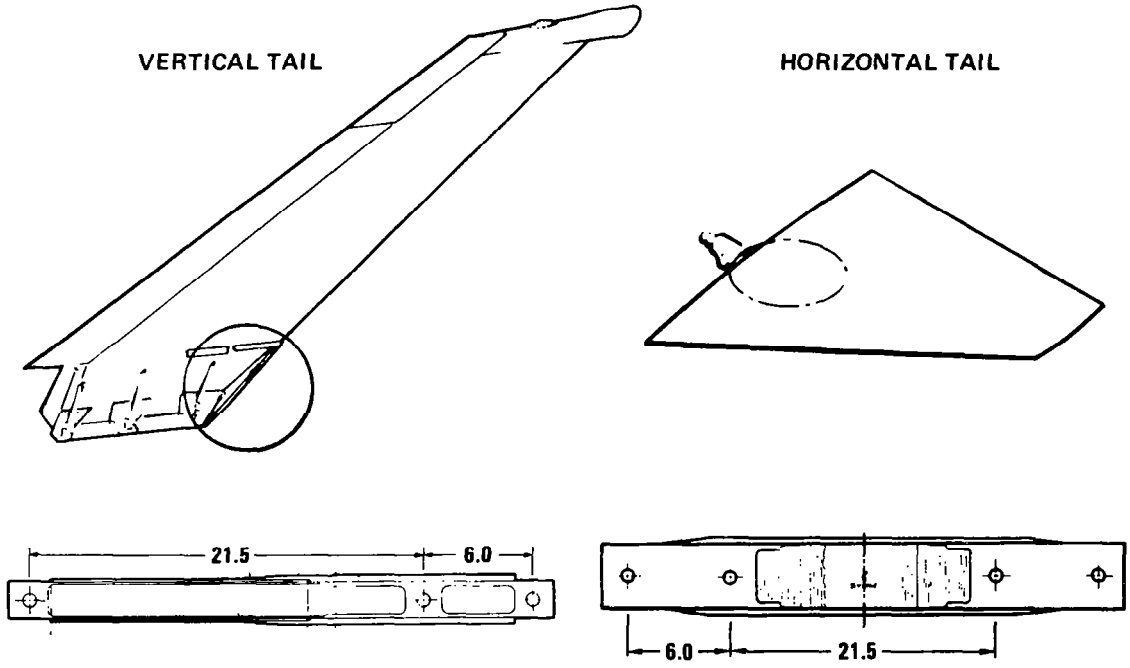

Figure 3

COMPOSITES ANALYSIS IS NECESSARY FOR TRACKING USAGE CHANGES

As we moved into Fleet Management activities, it became apparent that the design-usage-related test program was less than adequate for meeting the needs of the Air Force Logistics Command in terms of making maintenance decisions. And tests of each individual airplane/damage situation were out of the question. It was quickly concluded that composites analysis was necessary for tracking fleet and individual aircraft usage changes and to make repair decisions (Figure 4). Because few "zero-defect" parts are really built, the analysis must be able to relate defect size to time in service. The analysis should address the typical flaws occurring in manufacturing (durability flaws), those resulting from unusually bad manufacturing errors (damage tolerance flaws), and large damages occurring as a result of service usage. The issue is how these various flaws behave as a function of severe, normal, or mild usage of the airplane. The indicated relationship of flaw size to a buckling limit is illustrated in the following figure.

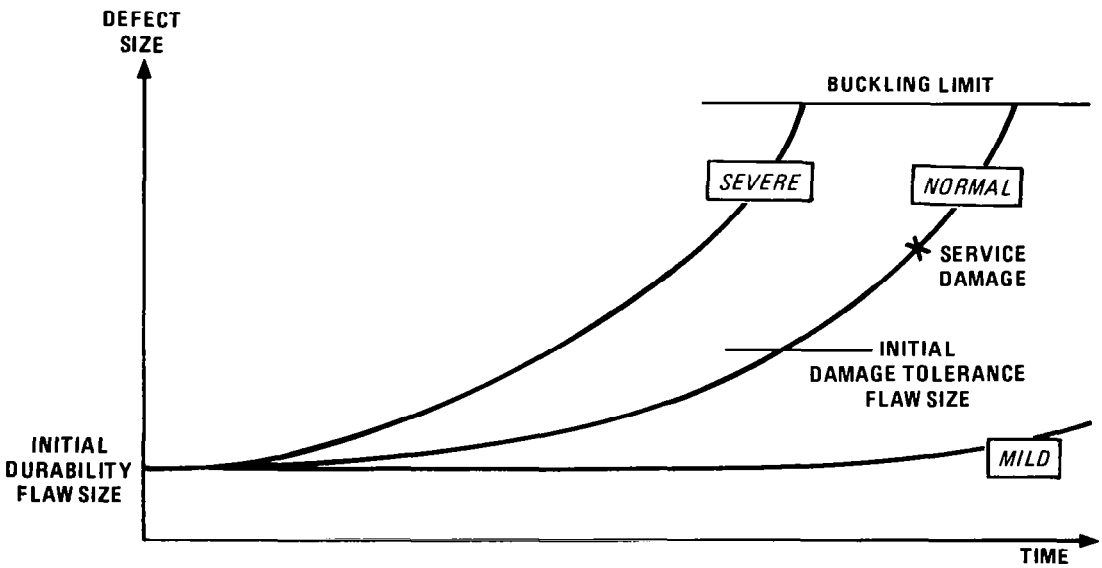

Figure 4

DELAMINATION IS MOST PREVALENT GROWTH MODE

In research work previously performed for the Air Force (Reference 1), we discovered that if any life-limiting, growth-related failure mode was likely to happen in a composite structure, it is probably delamination. Figure 5 shows about 15 inches of the overall 88-inch length of a box beam tested with a severe combination of bending and torsion. A delamination propagated in the compression surface skin until the surface finally buckled and caused the beam to fail. Some insight into the nature of delamination in graphite-epoxy can be obtained by exploring the toughness of some typical laminates in each of the three directions, as is outlined on the next chart.

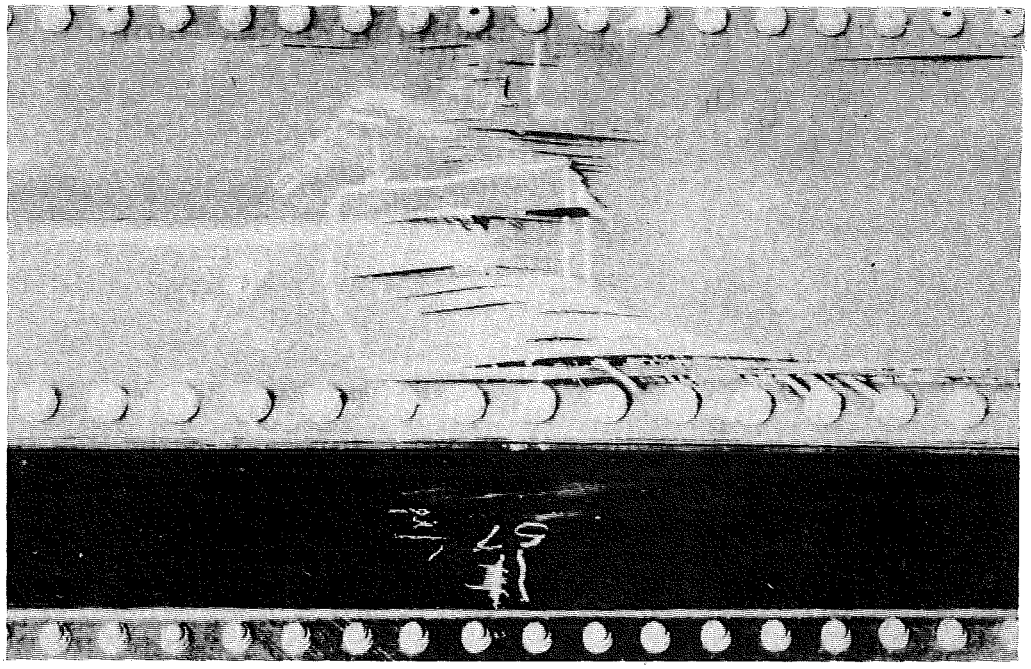

Figure 5

GRAPHITE-EPOXY FRACTURE TOUGHNESS

Figure 6, adapted from the results of Reference 2, plots fracture toughness (K_{IC} as measured by edge-notched beams or center-notched tensile coupons) as a function of the percentage of 0^{o} plies in a balanced, symmetric laminate containing only 0^{o} and $\pm 45^{o}$ plies of unidirectional tape. The trends are typical of the Thornel 300/Narmco 5208 class of graphite-epoxy, but the absolute numbers are not strictly valid because no ASTM standards have been developed for fracture toughness of composites. Nevertheless, we would agree that a $\pm 45^{o}$ laminate has a reasonable toughness slightly less than aluminum. As 45^{o} plies are replaced by 0^{o} plies, the toughness would be expected to increase until it was about doubled. On the other hand, as 45^{o} plies are replaced by 90^{o} plies, the toughness is expected to decrease until it reaches a minimum represented by a crack running completely in the resin between the fibers. The real point is that in the interlaminar mode, the toughness is always at the minimum.

These low values of interlaminar toughness are only significant as they relate to the out-of-plane loads discussed in the next chart.

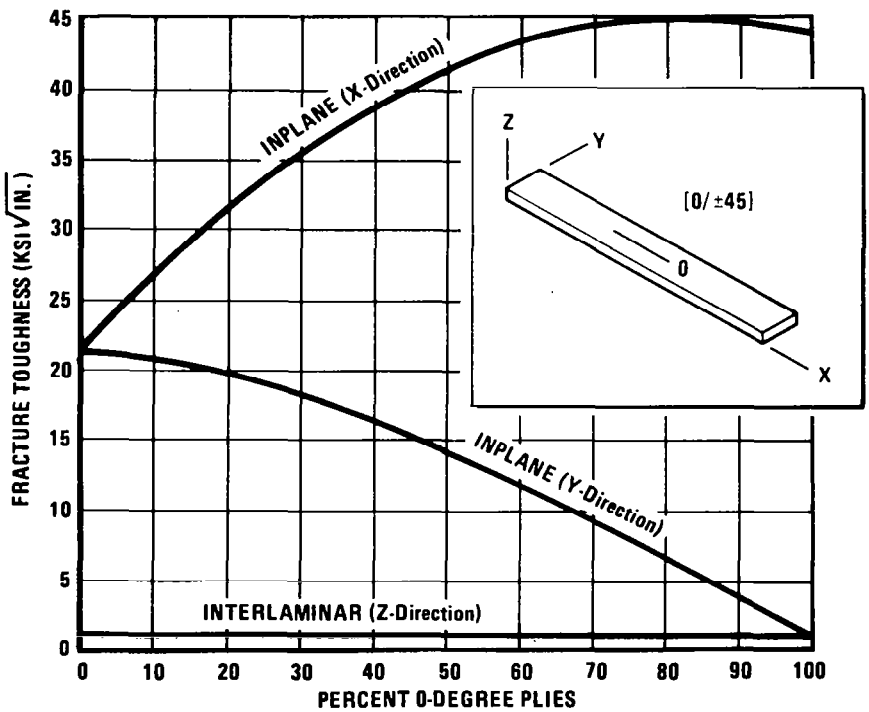

Figure 6

SOURCES OF OUT-OF-PLANE LOADS

Shown schematically in Figure 7 are five of the most common design details from which real hardware is constructed. Each of these details, even under in-plane loading, gives rise to interlaminar normal and shear forces. The interlaminar forces act directly on the plane of minimum toughness. As a result, delaminations may form, and if the in-plane forces are compressive, buckling becomes a pertinent issue.

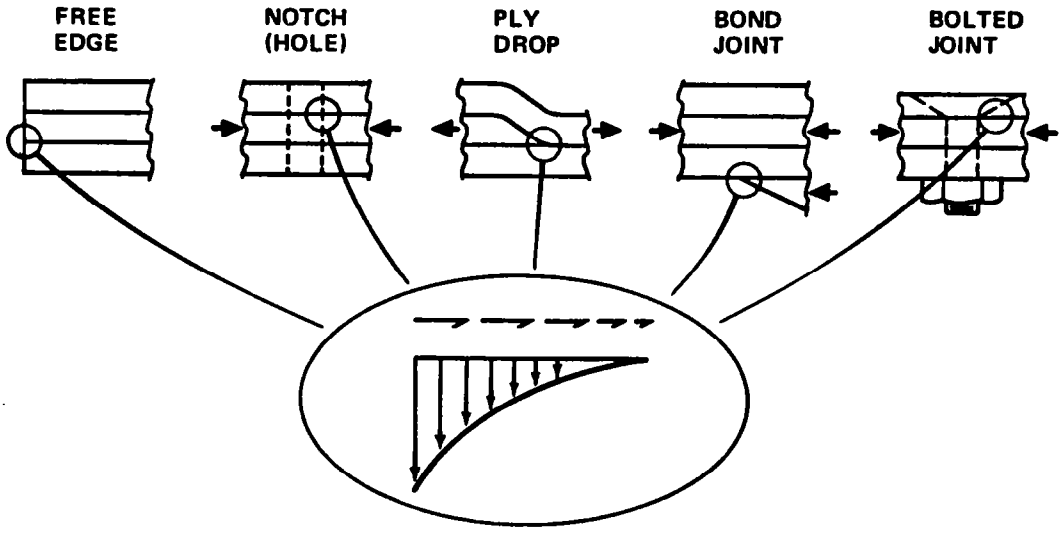

Figure 7

TRANSFORM THE PROBLEM

Creation of a compression coupon data base is impractical because interlaminar tension and shear interact with local and overall buckling so that specimen size, end conditions, and lateral support make scaleup difficult. A simpler, more direct approach (Figure 8) is to use an analysis to define the transfer function between applied loads and local rupture forces. Then the experimental effort can focus on tension and shear failure mechanisms.

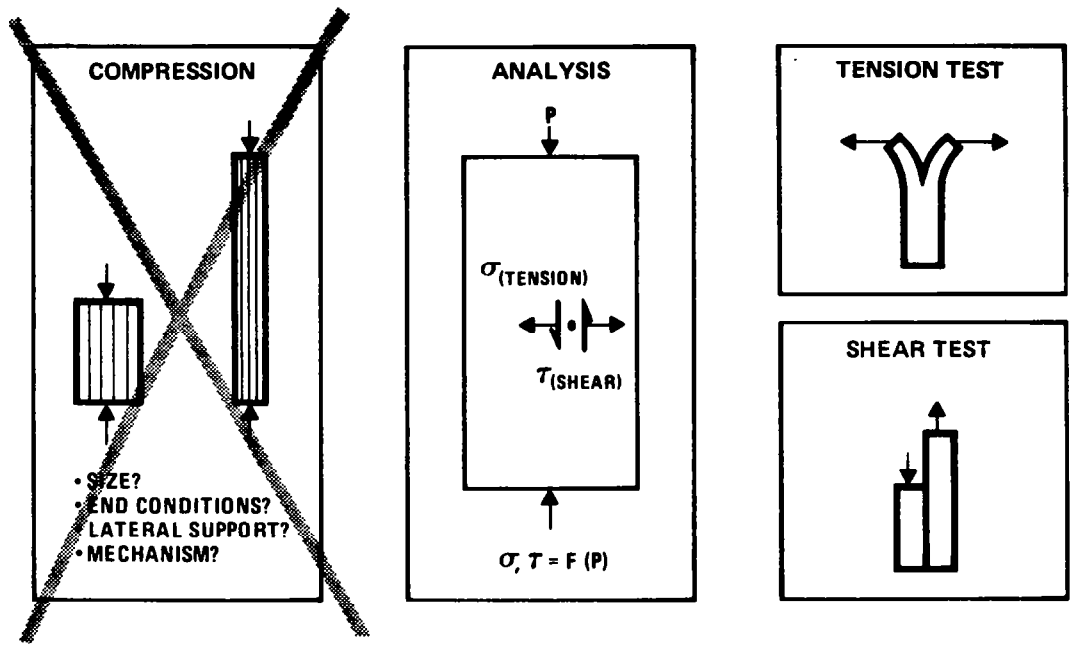

Figure 8

DELAMINATION ANALYSIS USES FRACTURE MECHANICS APPROACH

The capability is available from adhesive fracture technology (Reference 3) for computing the profiles of strain-energy release rate around a delamination in a laminated plate under general loading. As schematically depicted by Figure 9, the profiles can be broken into three components for use in a fracture-mechanics-based failure theory (such as Reference 4). The calculations can be performed with finite element methods coupled with the virtual crack closure technique (Reference 5).

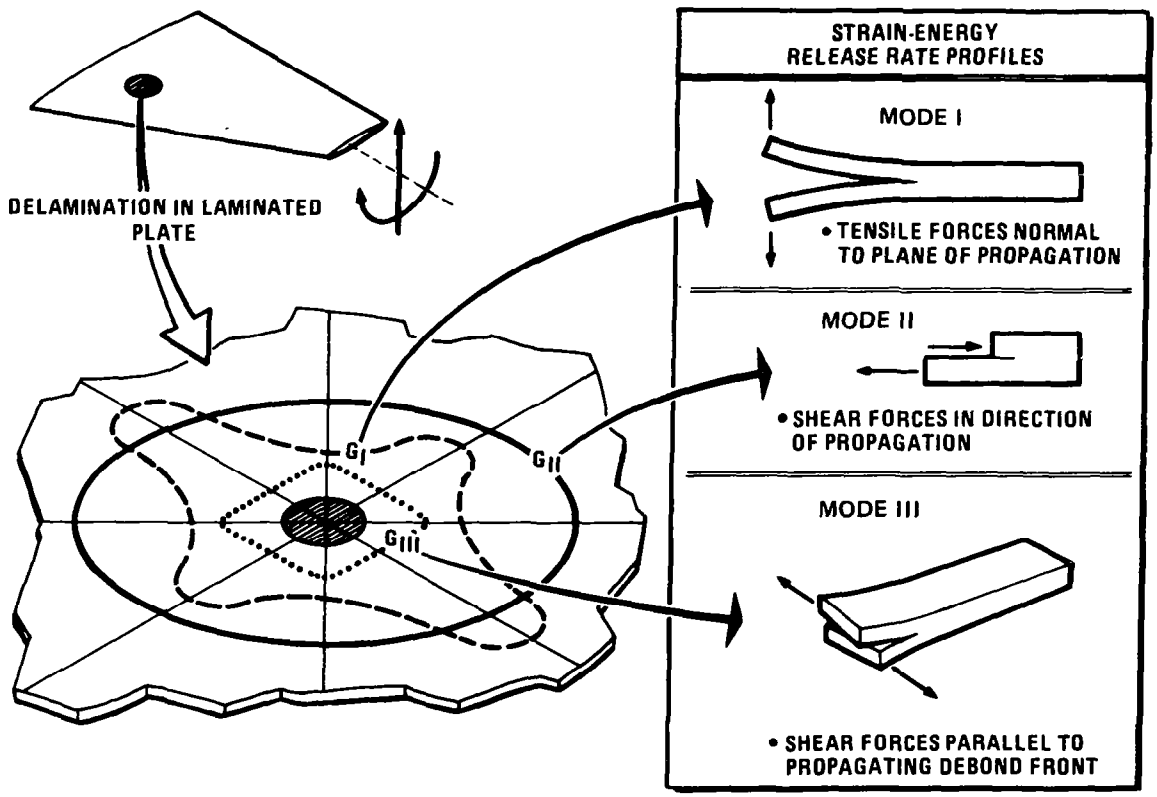

Figure 9

COMPOSITES DAMAGE TOLERANCE APPROACH

With this background, an approach (Figure 10) was taken for damage tolerance of composites on the F-16. Achievable goals were carefully set for this study by emphasizing manufacturing defects (such as planar voids) rather than service defects, concentrating on delamination as the major mechanism, developing a fracture-mechanics-based model, and doing it in five increasingly complex phases. The first three phases defined acceptable coupon test specimens, checked the influence of environmental effects, and sought a method for predicting unidirectional delamination growth under spectrum loads. The fourth phase was intended to extend the test base to limited two-dimensional growth in beam specimens representing thin and thick areas of the horizontal tail. Its results are not included in this presentation. Correlating delamination growth in a full-scale horizontal tail to that predicted by the coupons was the goal of the final phase.

- EMPHASIZE MANUFACTURING DEFECTS
- CONCENTRATE ON DELAMINATION
- DEVELOP A FRACTURE MECHANICS-BASED MODEL
- COMPLETE A 5-PHASE PROGRAM

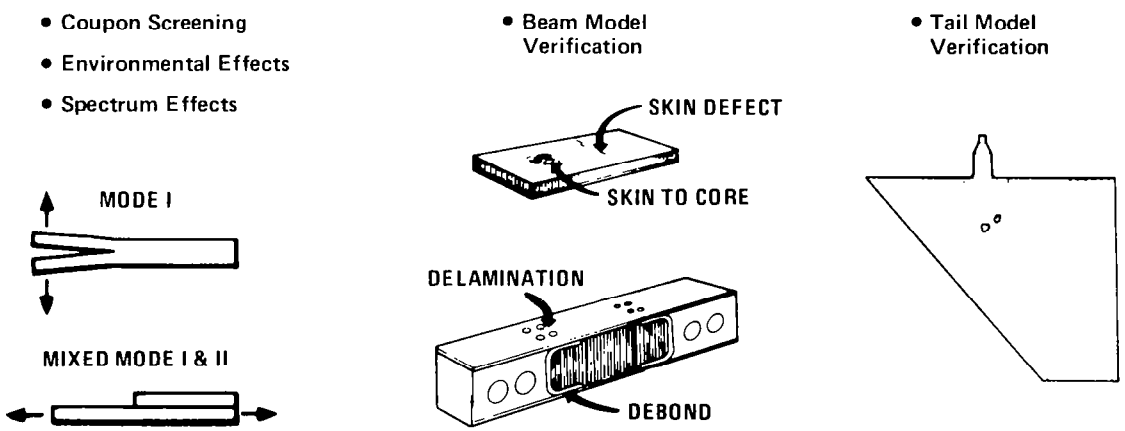

Figure 10

COUPON TESTS

The coupon test phases (Figure 11) were performed with a Mode I coupon and a mixed mode coupon with about 75% Mode II response. As reported in Reference 6, static tests produced the critical strain-energy release rates and their environmental behavior, and fatigue tests measured the delamination growth rates for constant amplitude and spectrum loading.

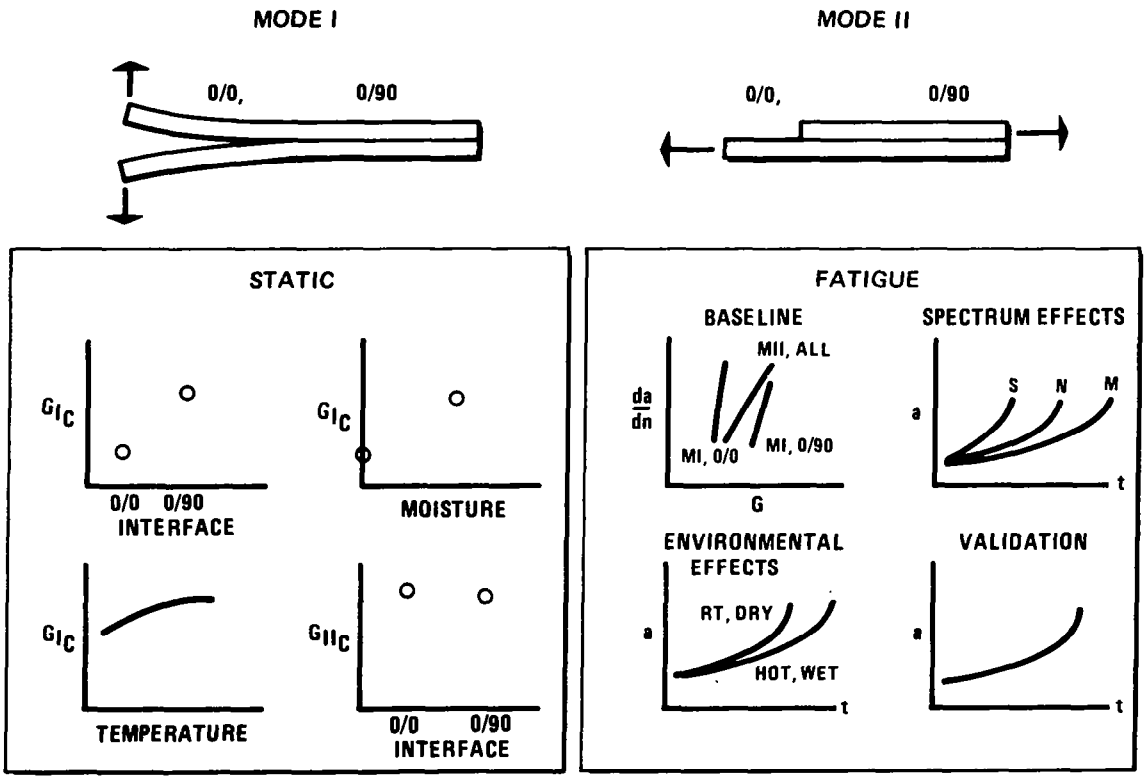

Figure 11

COUPON SUMMARY

Figure 12 outlines some of the important results of the coupon phases. These results have since been supplemented by the research reported in Reference 7.

- DEVELOPED UNIQUE TEST SPECIMENS AND METHODS
- MEASURED CRITICAL STRAIN-ENERGY RELEASE RATES
- FOUND GROWTH BEHAVIOR TO OBEY SIMPLE POWER LAWS
- CHECKED ENVIRONMENTAL EFFECTS
- PREDICTED SPECTRUM GROWTH ACCURATELY

Figure 12

TAIL MODEL VERIFICATION

An introduction for the final demonstration phase of the program is presented in Figure 13.

- OBTAIN A TAIL WITH KNOWN DEFECTS
- PERFORM FATIGUE TEST USING TRUNCATED SPECTRUM
- DO FRACTURE ANALYSIS
- CORRELATE MODEL TO GROWTH OBSERVATIONS

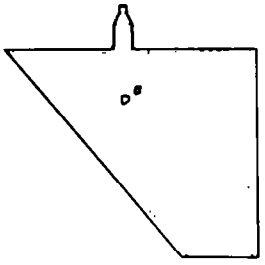

Figure 13

DEFECT LOCATIONS

Horizontal tail unit number 110 was selected for test and was brought back after 144 flight hours of normal service. One reason for its selection was that it contained a "corner defect," a 2.1-inch long by 0.3-inch wide delamination between the 51st and 52nd plies of the 52-ply graphite-epoxy skin, that had been repaired by injection of resin. Figure 14 shows the locations of the corner defect, the titanium hub-spar substructure, and the boundary of a ply termination separating the 12- and 10-ply thicknesses in the skin. In an area of high stress coinciding with the ply termination, two additional defects were introduced. One was an impact damage produced by dropping a 3.25-pound steel dart with a 1-inch-diameter hemispherical nose from a height of 2 feet. The other was a routed 3-inch hole in the skin down to the aluminum core, representing the clean-up hole around a typical skin repair that never got a patch bonded over it.

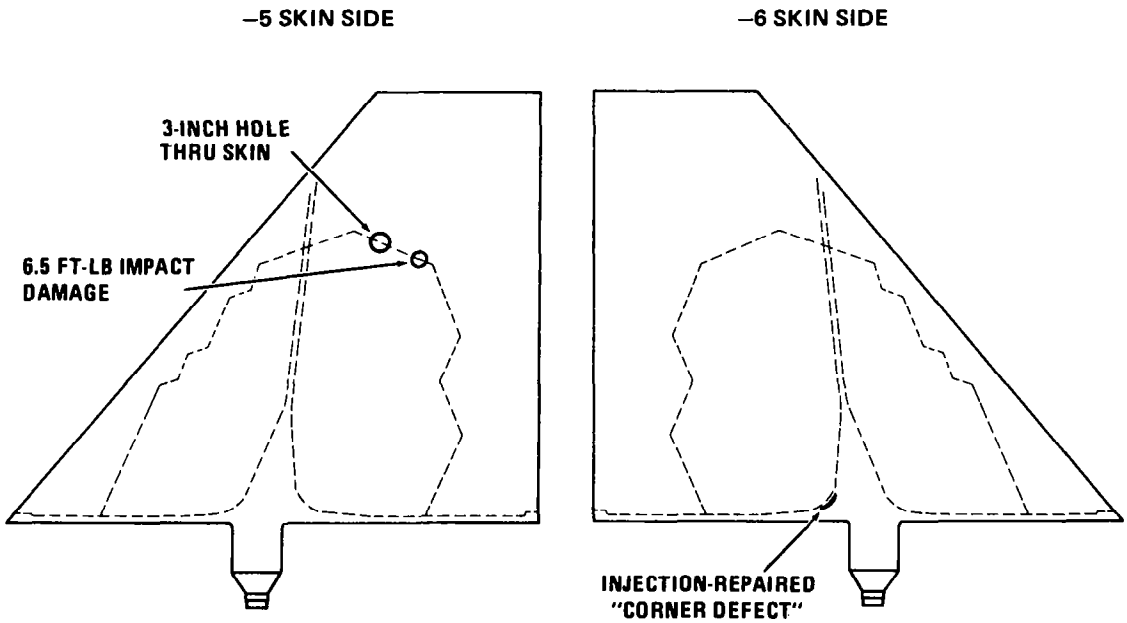

Figure 14

TAIL TEST HISTORY

The tail was tested in an air-conditioned lab environment. Figure 15 outlines the testing sequence.

- 1 LIFETIME OF DESIGN USAGE SPECTRUM LOADING
- 2 SPECTRUM REPETITIONS WITH LOADS MAGNIFIED BY 1.3
- 4162 FULLY REVERSED CYCLES OF 1.3 TIMES MAXIMUM SPECTRUM LOAD
- RESIDUAL STRENGTH TEST TO 246% DESIGN LIMIT LOAD

Figure 15

TAIL FLAW GROWTH

The overall views of both tail surfaces (Figure 16) show the outlines of delaminations created by the testing. The impact damage grew only slightly during the first few loads and exhibited no further growth. Delaminations grew from the 3-inch hole during the constant amplitude cycling. Large delaminations were produced in the root area of both surfaces. The first large increment of delamination at the 3-inch hole and at the root occurred during the first 2235 cycles of the constant amplitude cycling during which no inspections were made.

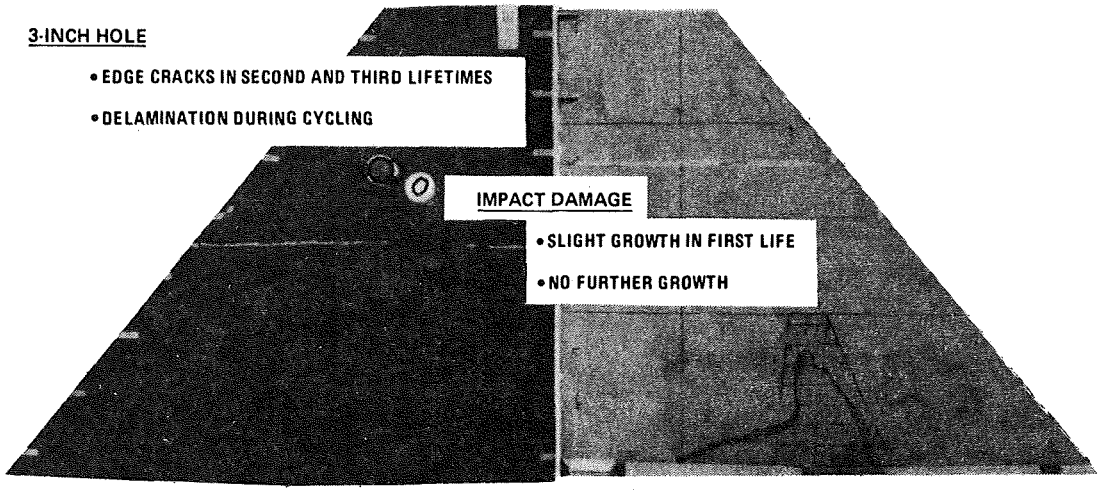

Figure 16

ROOT AREA MATH MODELS

The finite-element based fracture analysis used the "zoom-in" technique shown in Figure 17. Each succeeding detailed model was loaded with deflections from the previous model using MSC NASTRAN.

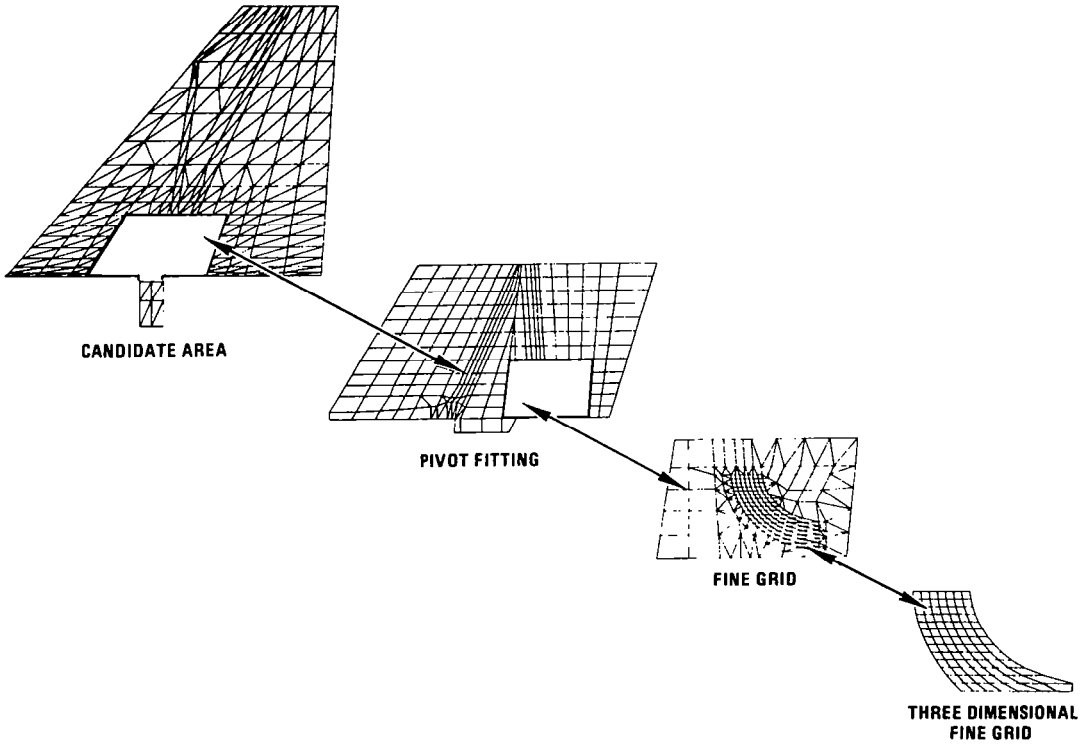

Figure 17

PLY CRACKING APPARENTLY TRIGGERED DELAMINATION

Figure 18 shows the 3-D brick model of the skin, substructure, and core in the local area of the "corner defect," as well as its top view and an internal view of the local geometry. The model showed a strong through-the-thickness stress concentration associated with the bonding of the skin to the titanium spar. Transverse stresses in the bottom +45° ply were much higher than the ply could carry, so its stiffnesses were modified to represent a cracked ply. Introduction of a delamination by releasing nodes as indicated gave a strain-energy release rate that was 90% of the critical static strain-energy release rate and thus was near the upper end of the delamination growth curve referred to in Figure 11.

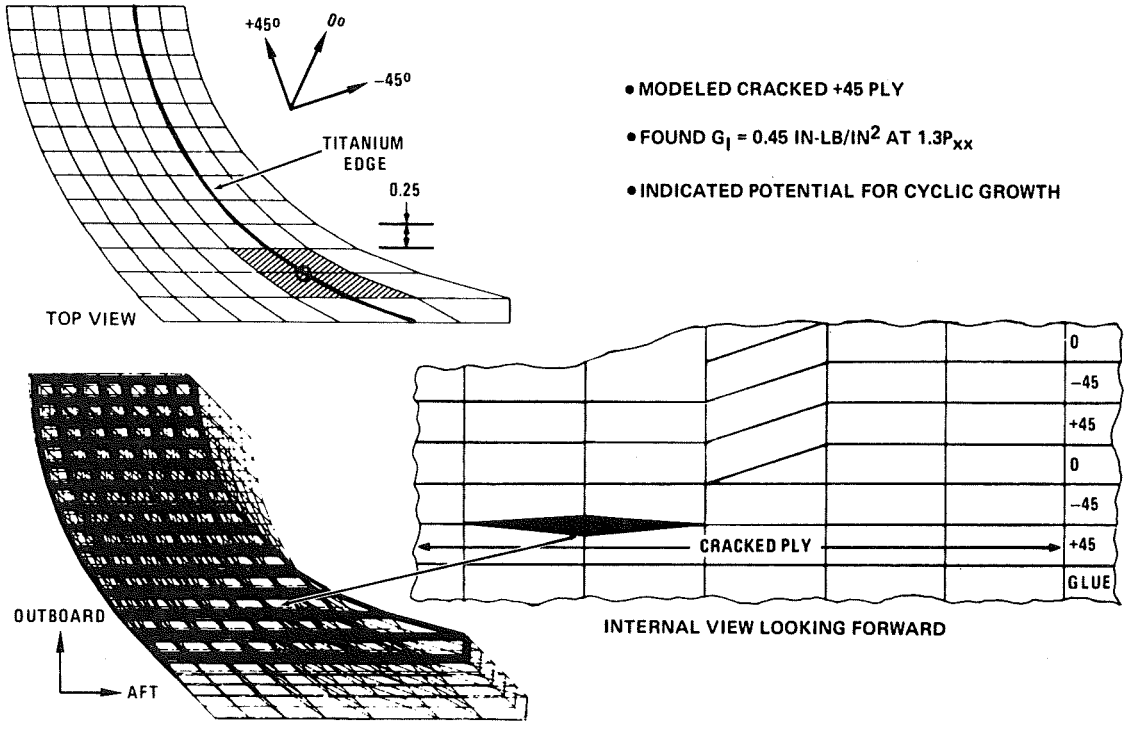

Figure 18

DELAMINATION GREW FROM 3-INCH HOLE

A closer view of the impact damage and 3-inch hole growth indications is presented in Figure 19, along with the number of fully reversed constant amplitude cycles associated with them.

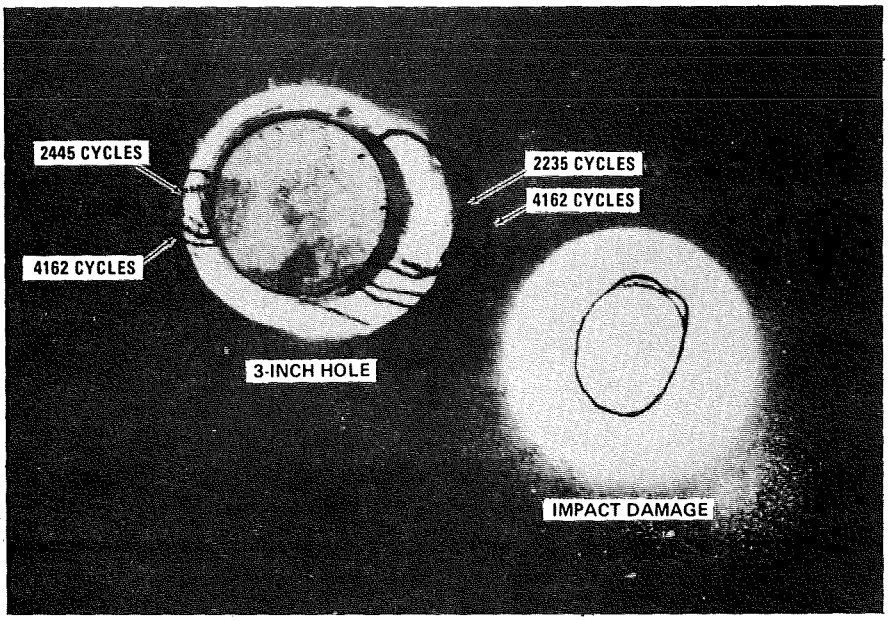

Figure 19

3-INCH HOLE MATH MODELS

Figure 20 depicts the "zoom-in" technique used for the 3-inch hole math models.

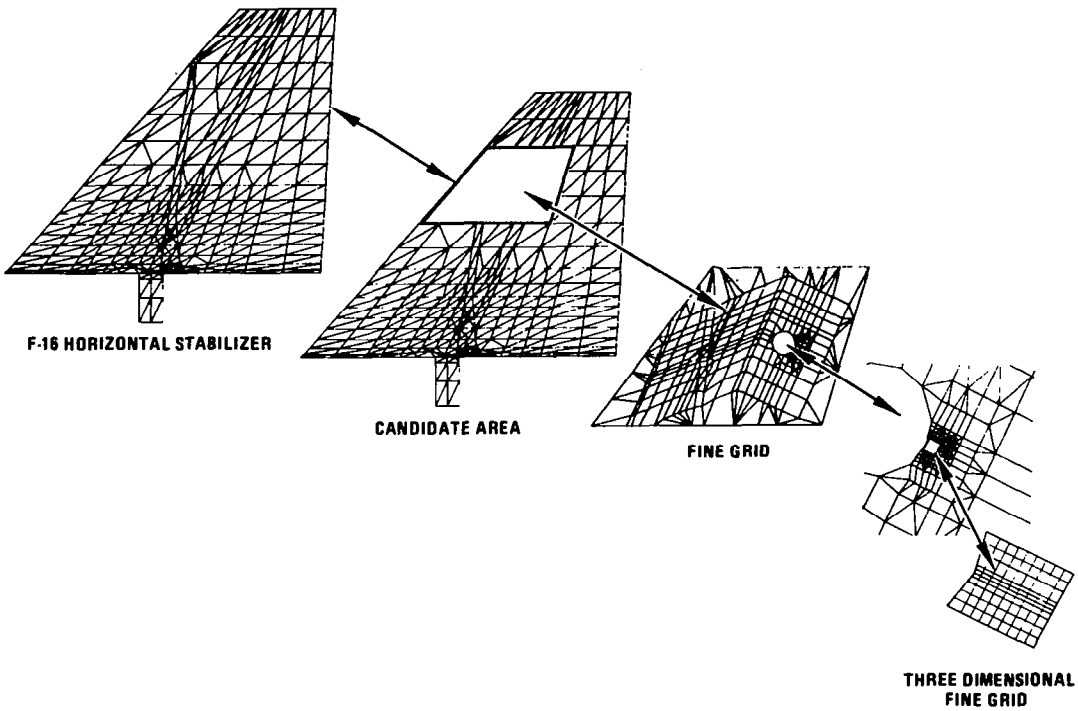

Figure 20

SEQUENCE OF CRACK ANALYSIS

The edge of the 3-inch hole is shown in Figure 21, along with the stacking sequence of the plies, all of which were modeled individually in the 3-D brick model. The model delamination was located between a -45^{o} ply and a 0^{o} ply. A node was released from the edge, then in all three possible directions, to indicate the preferred growth direction, which was along the ply termination. Succeeding nodes were released to "grow" the delamination.

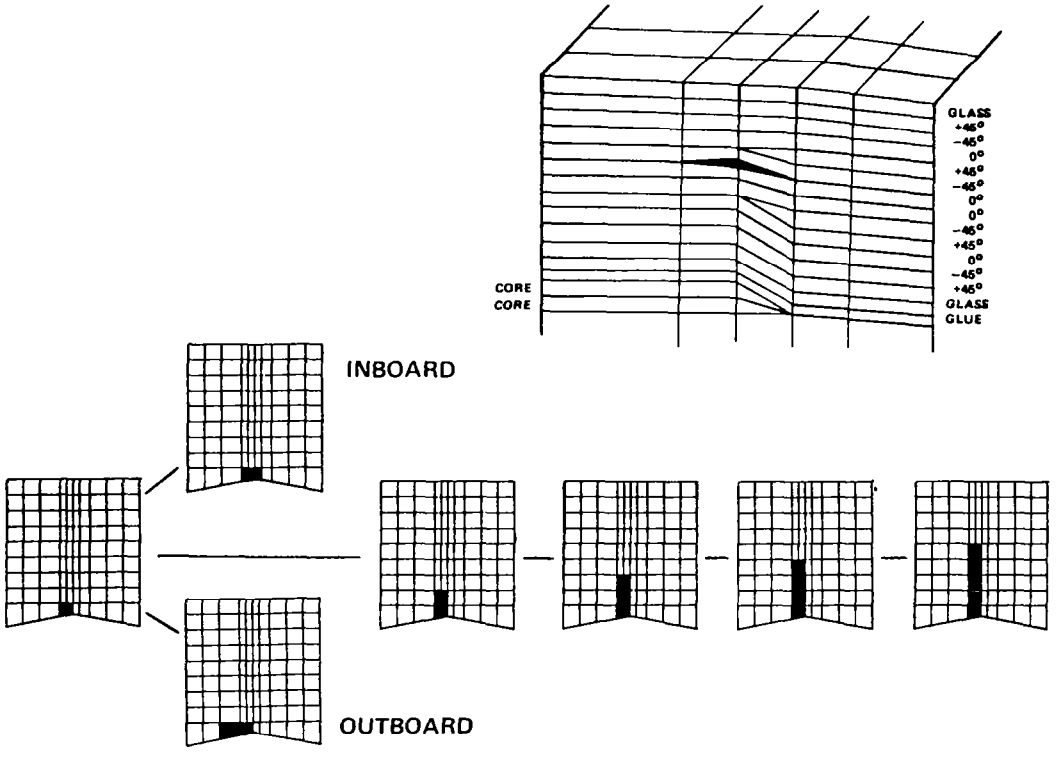

Figure 21

FRACTURE ANALYSIS AT P_{XX} LOAD

Results of the models, scaled to the peak load in the original design usage spectrum, are plotted in Figure 22. The analysis showed that a delamination of 0.085 inches should have resulted from that load. The plot of strain-energy release rate as a function of crack length was scaled to the square of the applied load and combined with the coupon static fracture and delamination growth rate data to produce the results shown in Figure 23.

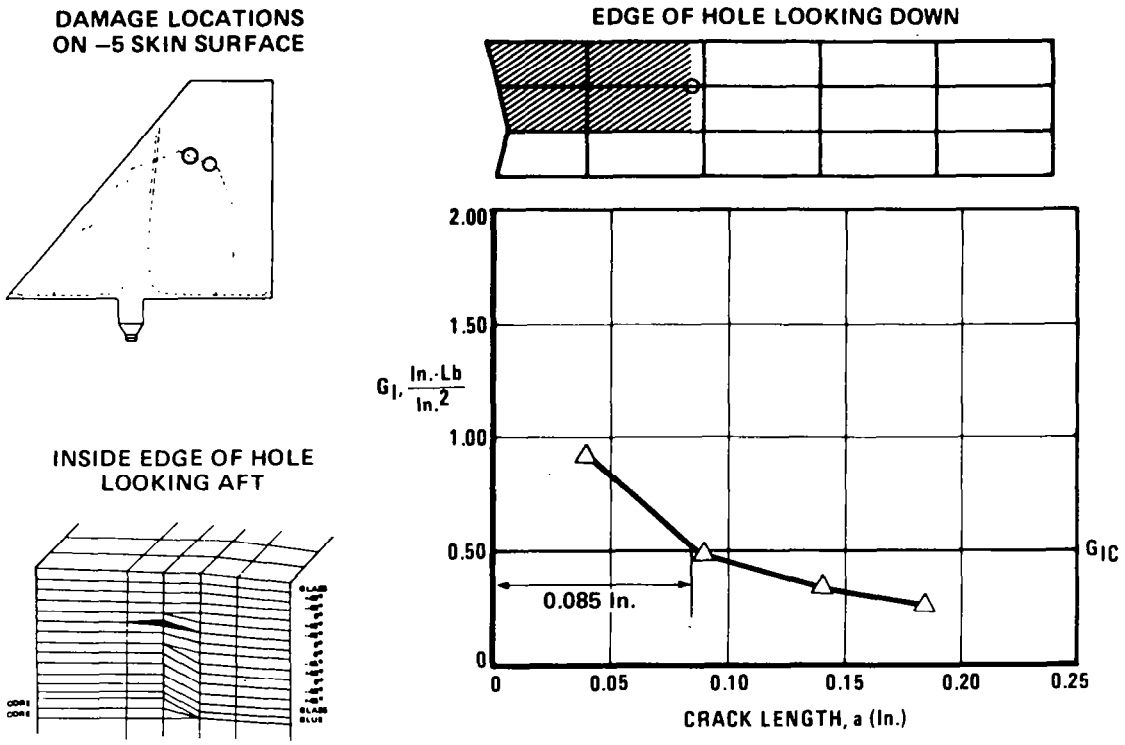

Figure 22

ANALYSIS AGREES WITH OBSERVED GROWTH

Figure 23 summarizes and correlates the growth calculations and observations. The resolution of the hand-held ultrasonic inspection technique at the edge of the hole was not good enough to locate the small delaminations predicted by the analysis. However, edge cracks were observed by surface replication of the cut surface of the hole. The agreement between calculations and measurements for the larger delaminations is quite satisfactory.

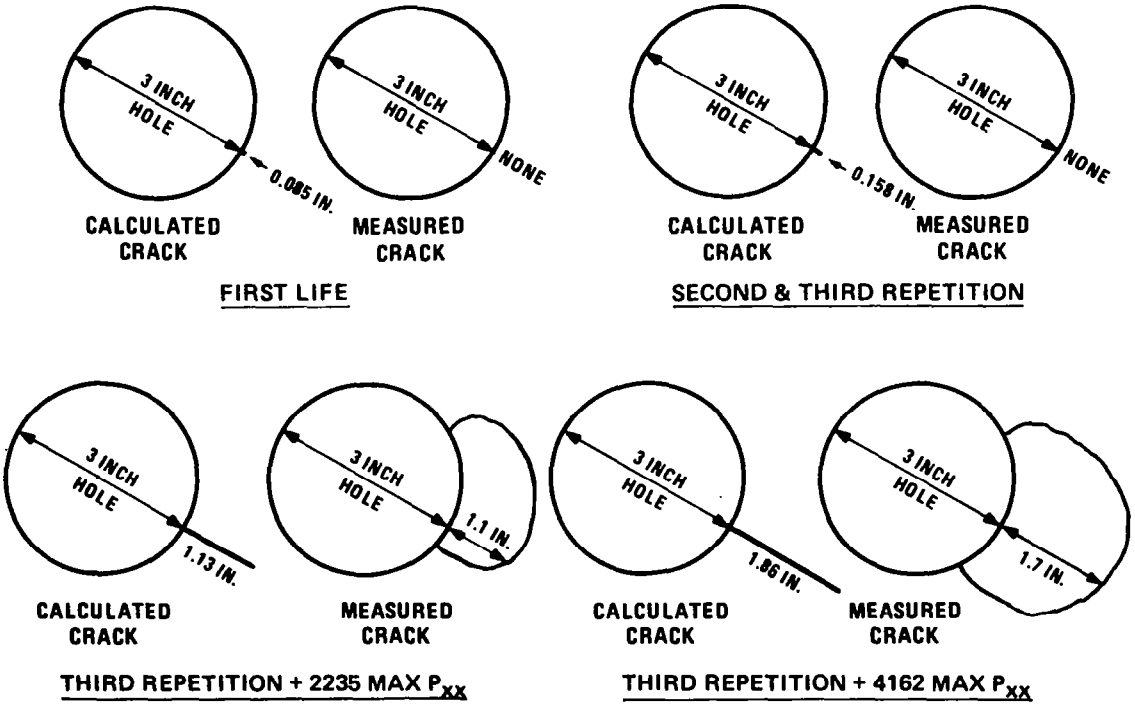

Figure 23

SUMMARY

The highlights of the program are reviewed and summarized in Figure 24.

COUPONS

- DEVELOPED UNIQUE TEST METHODS
- FOUND SIGNIFICANT DIFFERENCES BETWEEN PEEL & SHEAR
- PREDICTED SPECTRUM GROWTH

TAIL

- OBTAINED GROWTH ONLY UNDER EXTREME CONDITIONS
- DEMONSTRATED HIGH DAMAGE TOLERANCE
- SHOWED STABLE GROWTH IN REAL HARDWARE
- DEVELOPED MODELING PROCEDURE

Figure 24

The methodology, which General Dynamics believes to be equally applicable to both durability and damage tolerance analyses, is outlined in Figure 25. Its input is a flight-by-flight load history that is coupled to the fracture analysis to produce a sequence to strain-energy release rate/delamination size relationships. The coupon data base can then be entered to judge the potential for static or cyclic growth including the influence of moisture and temperature. A simple load-by-load growth model produces predictions of delamination size as a function of flight hours. This methodology has many attractive features, but the most important one is that it should be applicable to virtually any laminated composite structure.

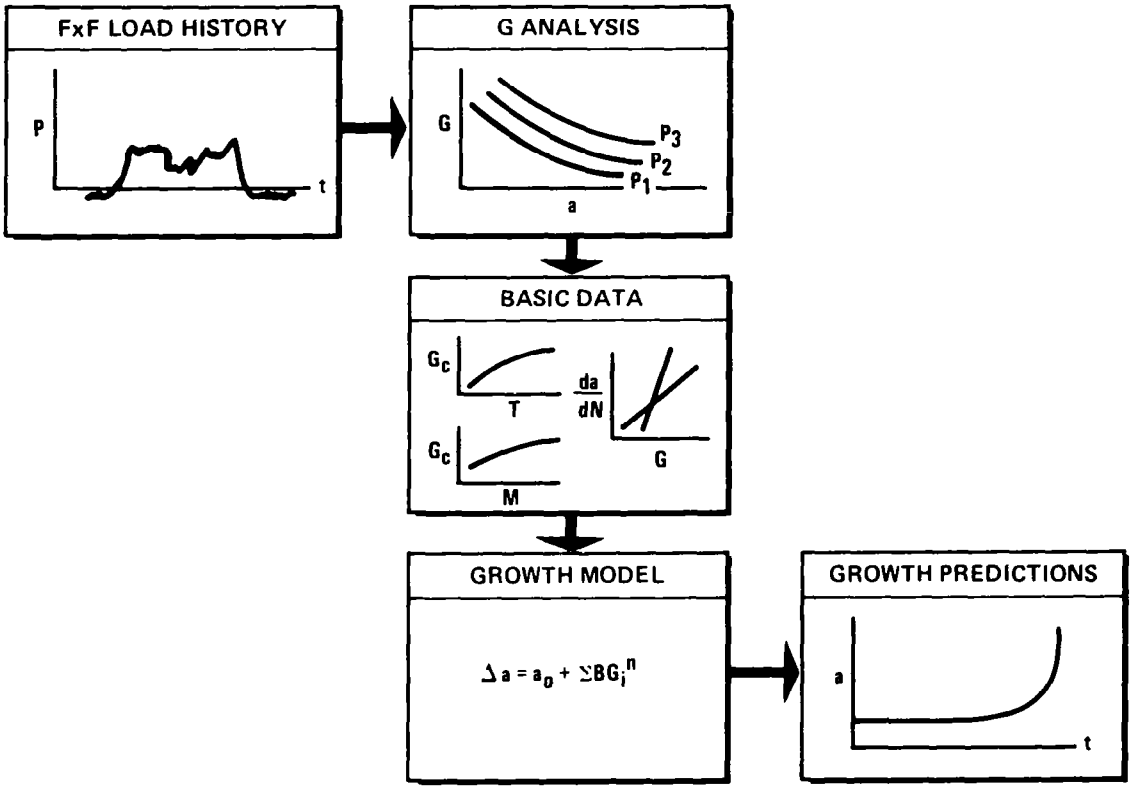

Figure 25

REFERENCES

1. Wolff, R. V. and Wilkins, D. J., "Durability Evaluation of Highly Stressed Wing Box Structure," Fourth Conference on Fibrous Composites in Structural Design, (San Diego, California, November 14-17, 1978), Plenum Press, 1980, pp. 761-770.

2. Konish, H. J., Swedlow, J. L., and Cruse, T. A., "Fracture Phenomena in Advanced Fiber Composite Materials," AIAA Journal, Vol. 11, 1973, p. 40.

3. Anderson, G. P., Bennett, S. J., and DeVries, K. L., Analysis and Testing of Adhesive Bonds, Academic Press, New York, 1977.

4. Wu, E. M., "Application of Fracture Mechanics to Anisotropic Plates," Journal of Applied Mechanics, Vol. 34, 1967, pp. 967-975.

5. Rybicki, E. F. and Kanninen, M. F., "A Finite Element Calculation of Stress Intensity Factors by a Modified Crack Closure Integral," Engineering Fracture Mechanics, Vol. 9, 1977, pp. 931-938.

6. Wilkins, D. J., Eisenmann, J. R., Camin, R. A., Margolis, W. S., and Benson, R. A., "Characterizing Delamination Growth in Graphite-Epoxy," Damage in Composite Materials: Basic Mechanisms, Accumulation, Tolerance, and Characterization, ASTM STP 775, American Society for Testing and Materials, 1982.

7. Wilkins, D. J., A Comparison of the Delamination and Environmental Resistance of a Graphite-Epoxy and a Graphite-Bismaleimide, Naval Air Systems Command Report NAV-GD-0037, September 15, 1981.